

Robot-Assisted Laser Strengthening: Mathematical Aspects

A. I. Gorunov^a, A. V. Kalyashina^{a, *}, and A. A. Gabitov^a

^aTupolev Kazan State Technical University—KAI, Kazan, Russia

*e-mail: anna_yik@mail.ru

Received November 15, 2018; revised November 20, 2018; accepted December 5, 2018

Abstract—A mathematical model is developed for predicting the surface characteristics of dies after laser strengthening by the Geksapod robotic system. The optimization of the laser-strengthening parameters is confirmed experimentally.

Keywords: laser beam, laser thermal strengthening, robotic system, mathematical model, optimization

DOI: 10.3103/S1068798X19070086

The thermal hardening of metals and alloys by laser radiation is based on local surface heating by the laser and rapid cooling as a result of heat transfer to inner layers of the metal. In other words, the heating and cooling times are small. As a result of thermal processes at the surface, a quenched zone with highly disperse crystalline structure and decreased etchability is formed. The depth of this zone depends on the power and radius of the laser zone, the time of laser action, and the thermophysical properties of the hardened material.

Laser surface hardening is intended to increase the wear resistance and working life of machine parts. It depends on highly concentrated radiation focused on a small area (between fractions of a millimeter and several mm).

The machining depth in surface quenching is generally 0.1–1.5 mm; for some materials, it reaches 2.5 mm. Relatively low beam power is used in hardening. That permits machining of the maximum surface area of the workpiece. As a rule, a rectangular laser spot is optimal.

The benefits of laser hardening include decrease in the additional machining required; the ability to treat nonuniform and thin workpieces and also those of complex shape; and machining of zones where heat supply is difficult in traditional methods and zones much smaller than the overall dimensions of the part. In view of the insignificant thermal influence on the workpiece as a whole, deformation is small. That eliminates or minimizes the need for further machining.

In the present work, we consider the mathematical aspects of laser thermal strengthening by means of a robotic system selected experimentally. First, the Geksapod manipulator with a smart control system is employed. The control system permits optimization of the treatment parameters (the displacement of the

laser spot relative the workpiece, its speed, the depth, and the temperature) and permits maintenance of the laser spot's speed on curvilinear sections of the die, ensuring constant parameters by feedback. To optimize the laser thermal strengthening, we use a robotic system that ensures stable machining parameters.

Laser thermal strengthening is especially effective in mass production and is widely used, for example, at OAO KamAZ, since it permits considerable savings of time. For instance, traditional strengthening of dies by nitriding takes 72 h. Around 900 dies of different type must be hardened, and the setup of the system must be changed for each die. Laser thermal strengthening eliminates the preliminary operations, without loss of product quality.

The new technology has been debugged in the experimental area at the KamAZ plant, using a robotic system with a Russian Geksapod manipulator.

THEORETICAL ASPECTS

The conditions of laser thermal strengthening are selected by determining the permissible ranges of the major parameters: the beam diameter, the machining speed, and the radiant power. The calculations are based on the method proposed in [1, 2]; we take account of the process parameters and the method employed.

Under the action of the laser, the metal surface absorbs only some of the radiation. We may write the effective absorption coefficient A_{eff} in the form

$$A_{\text{eff}} = 1 - R,$$

where R is the reflection coefficient.

Table 1. Chemical composition of 4Kh5MFS steel

C	Si	Mn	Ni	S	P	Cr	Mo	V
0.32–0.4	0.9–1.2	0.2–0.5	0.2–0.5	Up to 0.03	Up to 0.03	4.5–5.5	1.2–1.5	0.3–0.5

The power density of the laser with uniform distribution over the heating spot is

$$q = \frac{A_{\text{eff}}P}{\pi r^2}.$$

Here P is the power of the laser radiation; and r is the radius of the heating spot.

We assume that the intensity W_p of the laser is equal to the power density q with a uniform distribution over the heating spot and constant beam velocity v . The time t for which the heat source acts is determined as the ratio of the beam diameter to the relative velocity (the time for the beam to cover a path equal to its diameter)

$$t = \frac{2r_0}{v}. \quad (1)$$

Here r_0 is the radius of the beam.

If the heating depth satisfies the condition $z \ll 2\sqrt{at}$, we may write a simplified formula for the temperature, taking account of the time t for which the heat source acts and the heating depth z

$$T = \frac{W_p}{k} \left[\sqrt{\frac{4at}{\pi}} - z \right]. \quad (2)$$

Here W_p is the intensity of the heat source; k is the concentration of the beam; and a is the thermal diffusivity.

This simplification introduces an error no greater than 10% in the calculated temperature.

To take the influence of the simplification into account, we use a formula for the generalized velocity

$$\xi = \frac{vr_0}{2a}. \quad (3)$$

If $r_0 \gg \sqrt{at}$ or, equivalently, $\xi > 1$, the temperature may be calculated from Eq. (2).

The maximum attainable quenching depth z_q at the beam axis on surface heating without melting is

$$z_q = \sqrt{\frac{4at}{\pi}} - \frac{kT_q}{W_{p\text{eff}}} = \sqrt{\frac{4at}{\pi} \frac{T_{\text{me}} - T_q}{T_{\text{me}}}}, \quad (4)$$

where $W_{p\text{eff}}$ is the effective intensity of the heat source; T_q is the quenching temperature; and T_{me} is the melting point.

If we know the required quenching depth, which is specified in the design drawing as a rule, we may rear-

range Eq. (4) to find the time of action of the laser beam

$$t_q = \frac{\pi z_q^2}{4a} \left(\frac{T_{\text{me}}}{T_{\text{me}} - T_q} \right)^2. \quad (5)$$

The effective intensity of the heat source is found from the formula

$$W_{p\text{eff}} = \frac{k(T_{\text{me}} - T_q)}{z_q}.$$

Hence, we may write the radius of the focal spot required to ensure quenching depth z_q

$$r_0 = \sqrt{\frac{\gamma a P_0 z_q}{\pi k (T_{\text{me}} - T_q)}}, \quad (6)$$

where γ is a correction factor. Specifically, it is the ratio of the dimensionless temperatures calculated when the simplified and complete expressions are used for T_1 and T_2 .

If we know the beam's time of action and its radius, we may determine the relative velocity of the laser beam and the workpiece

$$v = \frac{2r_0}{t_q} = \frac{8a(T_{\text{me}} - T_q)^{3/2}}{\pi T_{\text{me}}^2 z_q^{3/2}} \sqrt{\frac{\gamma a P_0}{\pi k}}. \quad (7)$$

The width b_q of the quenched zone does not always correspond to the diameter of the focal spot. Depending on the thermophysical properties of the material, the heating time, and the intensity distribution, b_q may be larger or smaller than the focal spot, in accordance with the formula

$$b_q = 2r_0 \sqrt{1 - \left(\frac{T_q}{T_{\text{me}}} \right)^4}, \quad (8)$$

where T_{max} is the maximum temperature.

As a rule, b_q is specified in the design drawing. Therefore, it is expedient to determine r_0 from Eq. (8).

The results of calculations based on Eqs. (1)–(8) are as follows $t = 0.5$ s; $T = 1025^\circ\text{C}$, $\xi = 2.5$ m/s; $z_q = 0.78$ mm; $t_q = 0.49$ s; $r_0 = 2.2$ mm; $v = 9$ mm/s; $b_q = 4$ mm.

EXPERIMENTAL VERIFICATION

We produce a hard coating by laser thermal strengthening and, on that basis, verify the calculated parameters of the process.

The samples are made of 4Kh5MFS steel, whose chemical composition is summarized in Table 1.

We use a laser with diode pumping (wavelength 1064 nm; power up to 1000 W; beam velocity 9 mm/s). Using this system, the power of the laser radiation may vary from 800 to 2200 W. The other equipment employed is as follows: a robotic system based on a Geksapod manipulator with a smart control system [3]; an HX-1000TM hardness meter; and a universal microscope.

The steps in the experiment are as follows.

1. Preparation of Sample Surface

This step includes grinding; coarse and fine polishing; etching of microsections; measurement of the microhardness by means of HX-1000TM hardness meter; and analysis of the surface structure of metallographic samples by means of an Axiovert-200M inverted microscope.

The etch fluid consists of 15 cm³ HF; 35 cm³ HNO₃; 200 cm³ H₂O; and 100 cm³ glycerin.

2. Laser Thermal Strengthening

In laser thermal strengthening, we use the parameters calculated theoretically [4, 5].

The robotic system includes the Geksapod manipulator, an engineering viewing system, and a smart subsystem.

The Geksapod manipulator is of parallelepiped type, with six degrees of freedom. It ensures high machining precision and the required reproducibility of the parameters (Fig. 1).

The viewing system consists of a 3D laser scanner (precision up to 50 μm).

The smart subsystem is a computer module with software and electronic components, operating automatically.

A fiber laser with diode pumping is used as the tool head.

Additional software permits adjustment and training of the robot; simulation of its operation to assess the safety of the trajectory; adjustment and refinement of the technological conditions; visualization of the state of the system and the discrepancies; operation with the scanned models; and the production of 3D models of the samples.

A distinctive feature of the robotic system is that it permits simple and rapid adjustment of the machining process, under the direction of the technologist, on the basis of a 3D model of the workpiece. There is no need for precise positioning here. The system scans the workpiece, finds the corresponding 3D model, and by comparison, determines the machining area and conditions. That considerably abbreviates the setup time for a new product and the equipment downtime. Thus, the database may accommodate thousands of different parts, each of which the robotic system will

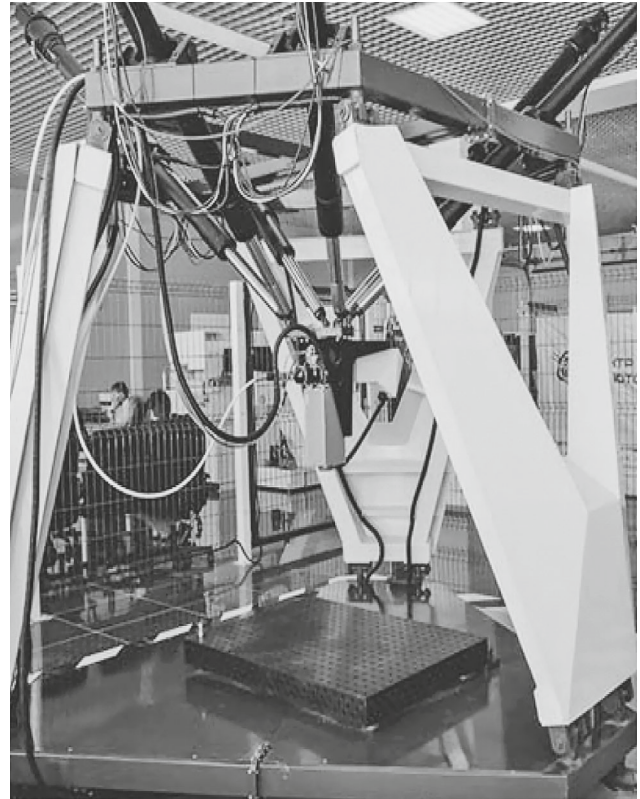


Fig. 1. Geksapod manipulator.

be able to identify. Depending on the particular part, the auxiliary equipment employed may be simple and universal or may be entirely unnecessary [4].

The benefits of the Geksapod manipulator are as follows [5].

(1) More rapid preparations for production and increased profitability because the machining, positioning, and measuring functions are combined in a single mechatronic complex.

(2) High precision in measurement and machining, thanks to the elevated (by a factor of five) rigidity of the rod mechanisms, the use of precision feedback sensors and laser measuring systems, and computer correction (for example, of the heat treatment).

(3) High speed: up to 10 m/s before machining and up to 2.5 m/s in machining.

(4) The absence of guides. Drive mechanisms serve as supporting elements of the structure. That improves its mass and size and decreases the consumption of materials.

(5) Standardization of the mechatronic components. That facilitates manufacture and assembly of the machine and also ensures design flexibility.

(6) Precise control of the motions, since the mechanisms are of low inertia, linear mechatronic modules

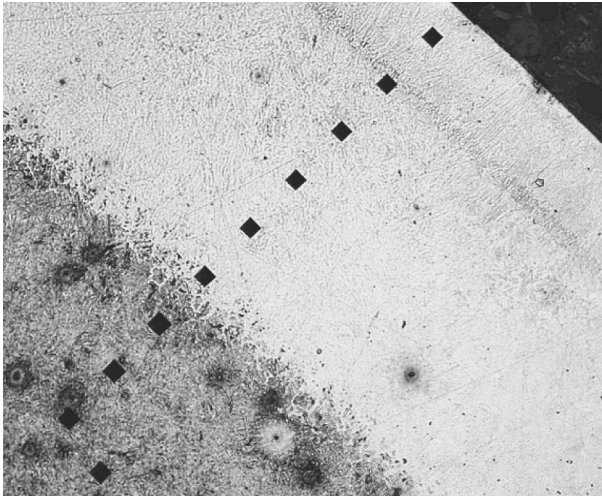


Fig. 2. Microstructure of quenched layer.

are regulated, and real-time methods of automated preparation and operation are employed.

3. Analysis of Samples after Machining

After laser thermal strengthening, samples are cut from the dies for metallographic analysis [6, 7]. The sample surfaces are ground and polished (in coarse and fine stages).

Nitric acid is used for etching of the microsections. The Rockwell hardness is measured by means of the HR150A instrument; and the microhardness is measured by means of the HX-1000TM instrument. The surface structure is determined by means of an Axiovert-200M inverted microscope.

4. Evaluation of the Results

After strengthening, three sections may be distinguished on the surface of the microsections.

(1) Ultradisperse structure: an unetched white layer consisting of fine martensite needles. The high rates of laser heating and subsequent cooling (by heat transfer to the interior of the metal) facilitate the creation of numerous crystallization centers and fixing of the consequent structure.

(2) A transition region, consisting of fragments of the initial structure, carbides, and some martensite.

(3) The initial structure (pearlite and carbides).

In Fig. 2, we show the cross section of the strengthened steel surface. After strengthening, we analyze the hardness distribution over the depth [8]. The distance between the markers identifying this distribution is 200 μm . The hardness is 59–61 HRC. We see that a hard unetched layer (depth 1 mm) with highly disperse structure is formed on the surface.

The parameters of laser strengthening are as follows:

Power of laser radiation, kW	0.4
Speed of laser spot over workpiece surface, mm/s	2
Scanning frequency, Hz	220
Flow rate of protective gas, t/min	3
Laser-spot diameter at workpiece, mm	2

On the basis of the experimental and calculated results for continuous laser thermal strengthening of 4Kh5MFS steel, we may determine the optimal parameters such that the mean depth of the hardened layer is increased when the width of the quenched zone is equal to the diameter of the laser spot.

The machining time for a batch of dies is determined experimentally (ten samples). The machining time is decreased by 18% when the robotic system is employed. In addition, the robotic system ensures uniform strengthening of dies of any shape and increases the hardness of the working surfaces to 60 HRC.

ACKNOWLEDGMENTS

Financial support was provided by the Russian Ministry of Education and Science (project 9.3236.2017/4.6) and by the Academy of Sciences (youth grant RT 03-64-ts-G-2018).

REFERENCES

1. Andriyakhin, V.M., Maiorov, V.S., and Yakunin, V.P., Calculation of surface quenching of ferrocement alloys using continuous-wave CO₂ lasers, *Poverkhn.: Fiz., Khim., Mekh.*, 1983, no. 6, pp. 140–147.
2. Gulyaev, A.P., *Metalovedenie (Metal Science)*, Moscow: Metallurgiya, 1986.
3. Andriyashov, V.A., Kalyashina, A.V., and Satdarov, T.R., Third-generation robotic complex for metal processing, *Vestn. Kazan. Nats. Issled. Tekh. Univ. im. A.N. Tupoleva*, 2015, no. 4, pp. 34–39.
4. Kalyashina, A.V. and Satdarov, T.R., Complex solution for the integration of a fiber laser and a third-generation robotic complex, *Fundam. Issled.*, 2016, no. 22 (4), pp. 730–735.
5. Gorunov, A.I., Laser hardening of 4X5MFS die steel, *Russ. Eng. Res.*, 2016, vol. 36, no. 3, pp. 206–208.
6. Maiorov, V.S., Parameter calculation of laser quenching with scanning, *Fiz. Khim. Obrab. Mater.*, 1989, no. 1, pp. 38–43.
7. Abil'sitov, G.A., Golubev, V.S., Maiorov, V.S., et al., *Tekhnologicheskie lazery. Spravochnik (Technological Lasers: Handbook)*, Abil'sitov, G.A., Ed., Moscow: Mashinostroenie, 1991, vol. 1.
8. Grigor'yants, A.G., Safonov, A.N., Maiorov, V.S., et al., Distribution of residual stresses on the surface of steels hardened with a continuous CO₂-laser, *Met. Sci. Heat Treat.*, 1987, vol. 29, no. 9, pp. 691–694.
9. Babitsky, V.I., Gerts, M.E., Ivanov, J.A., et al., US Patent 4795878, 1989.

Translated by Bernard Gilbert